1992

An analysis of anti reflective materials for the manufacture of semiconductor devices

Glenn A. Marshall
Lehigh University

AUTHOR:

Marshall, Glenn A.

TITLE:

An Analysis of Anti Reflective Materials for the Manufacture of Semiconductor Devices.

DATE: January 17, 1993

An Analysis of Anti Reflective Materials for the Manufacture of Semiconductor Devices

by

Glenn A. Marshall

A Thesis
Presented to the Graduate Committee
of Lehigh University
in Candidacy for the Degree of
Master of Science
in Electrical Engineering

Lehigh University

December, 1992

Certificate of Approval

This thesis is accepted and approved in partial
fulfillment of the requirements for the degree of
Master of Science

12/09/92
(Date)

Professor in Charge

Chairman of Department

Acknowledgments

Special thanks goes to my wife, Sharon whose patience and understanding through difficult times made my task much easier. In addition, thanks is extended to Dr. Charles Pearce for his assistance in identifying materials suitable for IC manufacturing. Finally, I would like to take the opportunity to thank all those at AT&T Microelectronics whose names are too numerous to mention but whose assistance has been invaluable.

Table of Contents

List of Figures

List of Tables

Abstract

Optical lithography performed on highly reflective surfaces limits the available image contrast provided by the exposure tool. Using a suitable anti reflective layer (ARL) enhances the reproducibility of optical images on such materials. This paper shows the results of a variety of such single layer AR systems for both a highly reflective and highly absorptive substrate. The theoretical results are based upon Fresnel equations and are compared to data collected from a spectrophotometer.

The introduction of the thesis shall contain preliminary information related to anti-reflective coatings and their importance to the manufacture of Integrated Circuits (IC's). This is followed by a discussion of ellipsometry and the manner in which optical coefficients are determined. Finally, an equation for percent reflection as a function of wavelength will be developed which is used to determine a theoretical model for each of the cases studied.

Experimentally, a variety of substrates were fabricated to determine the optimum characteristics of the ARL. Pure dielectric's as well as absorbing medium are manufactured using a variety of processes including substrate oxidation and sputter deposition. Data collection is performed by ellipsometry and reflectance spectroscopy. Where manufacture of the sample was not possible, theoretical data is substituted to illustrate substrate dependency.

In conclusion, actual results were compared against theoretical results and it was found that absorbing mediums are the best candidates for minimizing reflection on a highly reflective surface. In particular titanium nitride demostraates excellent properties in minimizing reflectnace at 436nm. The properties of the substrate have a great impact on the effectiveness of the ARL, especially in the case of dielectric materials. Overall, the theoretical calculations are very closely matched by the experimentally measured reflectance.

1.0 Introduction

1.1 The need for an ARL

Integrated circuit size constraints are largely dependent upon the limitations dictated by the lithographic process. With technology improving and line sizes going sub-micron, it becomes imperative to establish better ways to produce acceptable images. Photoresist patterns, though not entirely responsible, have a dramatic impact as to the integrity of the underlying structure. Utilizing an anti reflective layer (ARL) increases the available contrast of the system.

Ideally a non absorbing material with a deposited thickness equivalent to a quarter waveplate, on a perfectly reflecting substrate, will yield zero reflectance through phase cancellation. This only occurs if half of the available energy is reflected at the first interface and the remaining energy is not lost to the system. Unfortunately, this ideal system is not achievable with present day technology and therefore other considerations must be made. By incorporating a material with absorption properties not only reduces the reflectance but also creates a broader process window.

1.2 Development of Fresnel Coefficients

To best understand the principles of reflection this paper will start with the classical equations for electric and magnetic fields and develop them into equations for the reflection and transmission at an interface. For an isotropic medium the laws of electromagnetism are best represented by the following relationships

$$divD = \varepsilon divE = 4\pi\rho \tag{1}$$

$$divB = \mu divH = 0 \tag{2}$$

$$curlE = -\frac{\mu}{c}\frac{\partial H}{\partial t} \tag{3}$$

$$curlH = \frac{4E\sigma\pi}{c} + \frac{\varepsilon}{c}\frac{\partial E}{\partial t} \tag{4}$$

where these symbols have the standard definitions. For a medium in which there is no space-charge region, these relations are readily represented by Maxwell's Equations for electromagnetic radiation propagating through a medium.

$$\frac{\varepsilon\mu}{c^2}\frac{\partial^2 E}{\partial t^2} + \frac{4\pi\mu\sigma}{c^2}\frac{\partial H}{\partial t} = \nabla^2 E \tag{5}$$

$$\frac{\mu\varepsilon}{c^2}\frac{\partial^2 H}{\partial t^2} + \frac{4\pi\mu\sigma}{c^2}\frac{\partial H}{\partial t} = \nabla^2 H \tag{6}$$

By applying the appropriate boundary conditions it is possible to determine the amount of light reflected and transmitted at the interface of two different media. Incorporating these boundary conditions we obtain the following series of equations which can then be solved to yield the amplitudes of the transmitted and reflected vectors as related to the incident vectors.

$$\frac{E_{0p}^-}{E_{0p}^+} = \frac{n_0\cos\phi_1 - n_1\cos\phi_0}{n_0\cos\phi_1 + n_1\cos\phi_0} = r_{1p} \tag{7}$$

$$\frac{E_{1p}^+}{E_{0p}^+} = \frac{2n_0\cos\phi_0}{n_0\cos\phi_1 + n_1\cos\phi_0} = t_{1p} \tag{8}$$

$$\frac{E_{0s}^{-}}{E_{0s}^{+}} = \frac{n_0 \cos\phi_0 - n_1 \cos\phi_1}{n_0 \cos\phi_0 + n_1 \cos\phi_1} = r_{1s} \tag{9}$$

$$\frac{E_{1s}^{+}}{E_{0s}^{+}} = \frac{2n_0 \cos\phi_0}{n_0 \cos\phi_0 + n_1 \cos\phi_1} = t_{1s} \tag{10}$$

where E^- and E^+ denote the reflected and transmitted waves respectively. A graphical representation of the incident and reflected waves as related to equations 7 through 10 is shown in Figure 1.

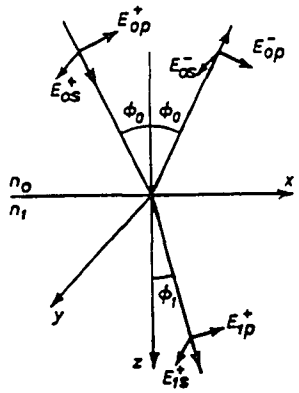

Figure 1 Vector diagram for reflection and transmission at an interface

For the case of normal incidence ($\phi = 0$) these equations reduce to the following

$$r_{1p} = \frac{n_0 - n_1}{n_0 + n_1} \qquad (11a) \qquad\qquad t_{1p} = \frac{2n_0}{n_0 + n_1} \qquad (11b)$$

$$r_{1s} = \frac{n_0 - n_1}{n_0 + n_1} \qquad (12a) \qquad\qquad t_{1s} = \frac{2n_0}{n_0 + n_1} \qquad (12b)$$

The values obtained r_{1p}, r_{1s} and t_{1p}, t_{1s} are known as the Fresnel coefficients for reflection and transmission respectively. The subscripts p (parallel) and s (perpendicular) referring to the plane of polarization are of no consequence to the results and therefore shall no longer be mentioned in this paper. As can be seen from the above equations $t = 1 + r$ and would indicate that when $n_0 > n_1$, the system generates energy which can not occur. This situation is rectified by applying Poynting's theorem and considering the energy within each medium. The Poynting

vector S which is the electromagnetic energy flux of the traveling wave, is defined as

$$S = \frac{c}{4\pi} n|E|^2 \tag{13}$$

where n is the refractive index for a non-absorbing medium. The reflectance and transmittance of the system is then given by

$$R = \frac{(n_0 - n_1)^2}{(n_0 + n_1)^2} \tag{14}$$

$$T = \frac{4 n_0 n_1}{(n_0 + n_1)^2} \tag{15}$$

For the case of an absorbing medium the refractive index is replaced by the complex index of refraction ($n \equiv n - ik$) where k is referred to as the absorption coefficient and yields the following equation for reflectance of the system

$$R = \frac{(n_0 - n_1)^2 + k_1^2}{(n_0 + n_1)^2 - k_1^2} \tag{16}$$

Since most of the media studied in this paper have an absorbing coefficient associated with them variations of equation 16 shall be used exclusively. For the special case of a single absorbing film on an absorbing substrate an adaptation developed by Heavens[1] is included in appendix A.

1.3 Scope of this thesis

The systems of interest in this paper are single layer mediums which incorporate a highly reflective substrate such as would be encountered with lithography on a metal film. Where manufacturing of the films is equipment limited, a silicon substrate is used to determine the materials' optical properties and then these properties are applied to the case of an aluminum substrate. For comparative purposes, all of the materials studied are also shown for the case of a silicon substrate.

2.0 Material Selection

2.1 The Substrate

In order to fabricate and analyze the materials contained in this paper two substrates possessing unique optical properties are employed. Since ARL's are typically used at metal layers to increase image integrity an aluminum alloy layer is used whenever possible. Due to equipment and process limitations a silicon substrate is also incorporated to study additional films. Once the optical parameters are determined for each substrate they are applied to the various systems under consideration.

2.2 The Anti reflective layer

The materials selected for this paper are intended to cover a broad range of conditions. Natural dielectrics, silicon dioxide and silicon nitride were selected because they absorb an insignificant amount of energy. Amorphous silicon has been an industry standard for many years and thereby provides a point of reference for the other materials effectiveness. Tantalum silicide and titanium nitride are also incorporated based upon work[2-3] previously done suggesting their usefulness as ARL's.

3.0 Experimental results

3.1 Fabrication

For this thesis, an array of substrates with specific optical properties are fabricated. Due to equipment limitations a variety of processing methods are utilized. The tantalum silicide is deposited using a Varian 3180 at a substrate temperature of 400C, an Argon ambient at 10mT creating a deposition rate of 40A/sec. The amorphous silicon is deposited also using a 3180 with the following process changes, the substrate bias temperature is 56C and an Argon ambient at 7.5mT which yields a deposition rate of 20A/sec. In both cases a power setting of 1.2kW is used and the substrate is flooded with Argon at a flow rate of 1.5mT to insure convection heating. The titanium nitride is reactively deposited using a Varian M2000 sputter deposition system, with a titanium target in a nitrogen and argon ambient. Due to the proprietary nature of the material additional information regarding the process is not available for publication. Thermal oxidation, for 1.1hrs at 920C in a dry oxygen environment is used to produce the silicon dioxide. The silicon nitride was deposited using a Low Pressure Chemical Vapor Deposition (LPCVD) system, at a process temperature of 800C and in a dichlorosilane and ammonia ambient for 15.5min. this achieves a deposition rate of 35A/min. Creation of the extremely thin conductive and amorphous silicon layers is achieved by depositing a thicker more accurately measurable layer and then scaling down the deposition time accordingly. More precise measurements are achieved using Transmission Electron Microscopy (TEM) and are the values shown in the accompanying table. A Nanospec model 210 was used to measure the thickness of the dielectric materials. Material compositions for each of the samples whether manufactured or theoretical are summarized in tables 1 and 2 respectively.

Substrate	Film(s)/Thickness
Silicon	SiO_2 / 750 $\mathring{A}$
Silicon	Si_3N_4 / 550 $\mathring{A}$
Aluminum	TiN / 350 $\mathring{A}$
Aluminum	$\alpha - Si$ / 150 $\mathring{A}$
Aluminum	$TaSi_2$ / 100 $\mathring{A}$

Table 1 Manufactured film compositions and thicknesses

Substrate	Film(s)/Thickness
Aluminum	SiO_2 / 750 $\mathring{A}$
Aluminum	Si_3N_4 / 542 $\mathring{A}$
Silicon	TiN / 350 $\mathring{A}$
Silicon	$\alpha - Si$ / 150 $\mathring{A}$
Silicon	$TaSi$ / 100 $\mathring{A}$

Table 2 Film compositions studied based on material properties

3.2 Ellipsometer Measurements

The angles Δ and Ψ, known as the phase change and relative amplitude attenuation respectively, are required to determine the films optical coefficients. Using both a Rudolph Research AutoEL IV and AutoEL II ellipsometer with the following conditions. The angle of incidence (Φ) on both systems is fixed at 70 degrees[4]. The AutoEL IV utilizes a high pressure mercury lamp and a set of matched filters and analyzers at wavelengths of 365nm, 405nm and 546nm. A Helium-Neon laser is used by the AutoEL III which allows for data collection at 632nm. With the wavelength and angle of incidence known, the ellipsometer can then determine the values for Δ and Ψ. The values of Delta and Psi, corresponding to each of the materials at these wavelengths are summarized in tables 3 and 4 respectively.

	Wavelength (nm)			
	365	405	546	632
Aluminum	42.47	42.36	41.86	41.43
α-Silicon	23.71	21.39	16.61	13.54
Silicon	26.69	19.49	12.11	10.43
Tantalum Silicide	24.82	24.49	23.46	22.70
Titanium Nitride	15.61	15.07	19.27	24.18

Table 3 Psi values in degrees from ellipsometer

	Wavelength (nm)			
	365	405	546	632
Aluminum	110.34	115.95	129.62	135.31
α-Silicon	129.10	135.3	149.23	162.51
Silicon	158.35	172.76	174.70	175.20
Tantalum Silicide	122.76	127.1	136.04	138.09
Titanium Nitride	96.44	93.31	82.70	86.6

Table 4 Delta values in degrees from ellipsometer

3.3 Spectrophotometry

Once the optical properties of the materials are determined it is possible to have a suitable compound manufactured and tested. Testing is accomplished using a Perkin-Elmer UV/VIS/NIR spectrophotometer, which is capable of covering wavelengths from 180nm to 3200nm, this paper however has limited the range to the 300nm to 600nm regime. In order to cover this wide range the system utilizes a series of lenses and two unique light sources, a Deuterium lamp for the UV spectrum and a Halogen lamp for the visible spectrum. Determination of this range is governed by the wavelengths available for the ellipsometers. The system is set-up such that the incident beam is at an angle of 6 degrees off normal[5] , and although this results in some scattering of the incident beam at the boundaries, is considered to be inconsequential for our purposes.

4.0 Results

4.1 Calculated values

The Delta-Psi measurements collected were used to calculate[1] the refraction and absorption coefficients for the materials of interest, these values are listed in tables 5 and 6 respectively. Using these wavelength dependent properties linear regression was used to develop an equation (table 7) for each complex film studied. This information is then utilized to determine the theoretical response of each film and is plotted on the same graph as the experimental data for ease of comparison, see figures 2 through 6.

	Wavelength (nm)			
	365	405	546	632
Aluminum	.358	.431	.781	1.089
α-Silicon	3.32	3.75	4.15	4.141
Silicon	6.156	5.419	4.09	3.86
Tantalum Silicide	3.008	3.232	3.846	3.927
Titanium Nitride	2.482	2.441	2.019	1.766
Silicon Dioxide	1.47	1.46	1.46	1.46

Table 5 Refractive indices calculated from Delta-Psi values

	Wavelength (nm)			
	365	405	546	632
Aluminum	3.568	3.989	5.319	6.118
α-Silicon	2.679	2.329	1.325	.671
Silicon	3.043	.542	.160	.115
Tantalum Silicide	2.773	2.794	2.704	2.557
Titanium Nitride	1.333	1.254	1.370	1.715
Silicon Dioxide	0	0	0	0
Silicon Nitride	0	0	0	0

Table 6 Absorption coefficients calculated from Delta-Psi values

[1] See Appendix B for a sample calculation

Aluminum	$n(\lambda) = (.003\lambda - .67) - (\exp(.002\lambda + .574))i$
α-Silicon	$n(\lambda) = (.003\lambda + 2.365) - \exp(-.005\lambda + 2.861)i$
Silicon	$n(\lambda) = (-.009\lambda + 9.036) - (\exp(-.011\lambda + 4.468))i$
Tantalum Silicide	$n(\lambda) = (.004\lambda + 1.772) - (\exp(-.0003\lambda + 1.141))i$
Titanium Nitride	$n(\lambda) = (-.003\lambda + 3.524) - (\exp(.000935\lambda - .113))i$

Table 7 Summary of substrate reflection equations

4.2 Analysis

As can be seen from figures 2 through 6 the experimental data agrees to within a few percent of the theoretical values, indicating that the functions derived for each of the films are valid for this range of wavelengths. Figures 7 and 8 which compare the ARLs' effectiveness for both the aluminum and silicon substrates respectively show explicitly the substrate dependency. Dielectric materials, silicon nitride in particular, which is well suited for silicon applications, is of little value when used in conjunction with a highly reflective surface. Reflectance from the uppermost surface appears to govern the reflectance observed for the tantalum silicide, indicating that though a fraction of the wavefront is transmitted into the medium it is completely absorbed while traversing the film. The α-silicon provides adequate reflectance reduction in addition to a rather broad operating range when applied aluminum as should be expected when deposited on single crystal silicon has little impact as an absorber. Providing an even greater process window on aluminum, the titanium nitride not only exhibits excellent reflective properties but reportedly[6] eliminates the need for removal at metal levels due to its' electrical properties. As shown in figure 8 the minimum reflectance for the amorphous silicon occurred at $500\mathring{A}$. Intuitively, it would appear that simply by decreasing the thickness of the ARL, the minimum of the system would also shift however, this is not the case for this system. As we can see from figure 9, reflectance for a wavelength of 436nm is minimizes at approximately $160\mathring{A}$. The absorbing medium and substrate combination, as shown in figure 10 for amorphous silicon, illustrates that although a minimum is achieved at 436nm for a thickness of $110\mathring{A}$ it is not the absolute minimum as previously determined. Figure 11 which shows a similar upward shift in minima is still a highly effective system. These two systems clearly indicate that selecting an appropriate AR material is not a trivial matter and should be analyzed from all possible directions.

5.0 Discussion

The optical properties discussed in this paper were achieved using the process variables included in the experimental section. These properties varied significantly with work previously done in the field of anti reflective materials. One such example is the response of the Tantalum Silicide, in the works of C. Nolscher, L.Maden and M. Schneegans[6] they reported a refractive index of $n=3.85 - 2.03i$ and were able to produce a suitable film for use as an ARL. Figure 12 shows a comparison of the experimental results and their theoretical model as applied to the aluminum substrate studied in this paper. This figure indicates that although they were able to produce an acceptable ARL, differences in processing and/or substrate properties kept us from achieving the same. In addition it has previously been reported[7] that for classical metals $n=k$, this is clearly not the case as determined in this work.

Classical quarter waveplate cancellation is not useful when dealing with highly reflective materials, unless you have an absorbing component in the system. However, as demonstrated by the tantalum silicide excessive absorption negates the effect of the quarter waveplate and therefore must be considered carefully.

6.0 Future Work

Additional program development for complex refractive indices needs to include, the determination of the optimum ratio for n / k so that the stoichiometry of the films may be varied to yield a more suitable material.

Continued work is also needed in identifying additional materials which would not only simplify the manufacturing process but have no adverse impact on the performance of the circuitry.

7.0 Conclusions

A variety of anti reflective materials were analyzed in order to determine the most desirable properties of such films. This paper clearly demonstrates that total system reflectance is highly substrate dependent. Most notable is the behavior of silicon nitride which when deposited on silicon exhibited a very desirable ARL however, in the case of aluminum as a substrate it had an exceptionally high reflectance at its minimum. Materials with an absorbing coefficient allow for greater process latitude on highly reflective surfaces by not only reducing the reflectance but also by widening the trough.

Since ARL's are required primarily at the latter processing levels, the dielectric materials which possess excellent properties on silicon are of little value from the time the first metal layer is deposited, as demonstrated by their poor performance on aluminum. Amorphous silicon having been incorporated for many successful years appears to be sufficient as an ARL but, in reallity becomes less effective as the wavelength is decreased. With advantages in step reduction and increased process latitude the titanium nitride appears best suited as an ARL by allowing for the greatest process latitude and the least reflection at 436nm.

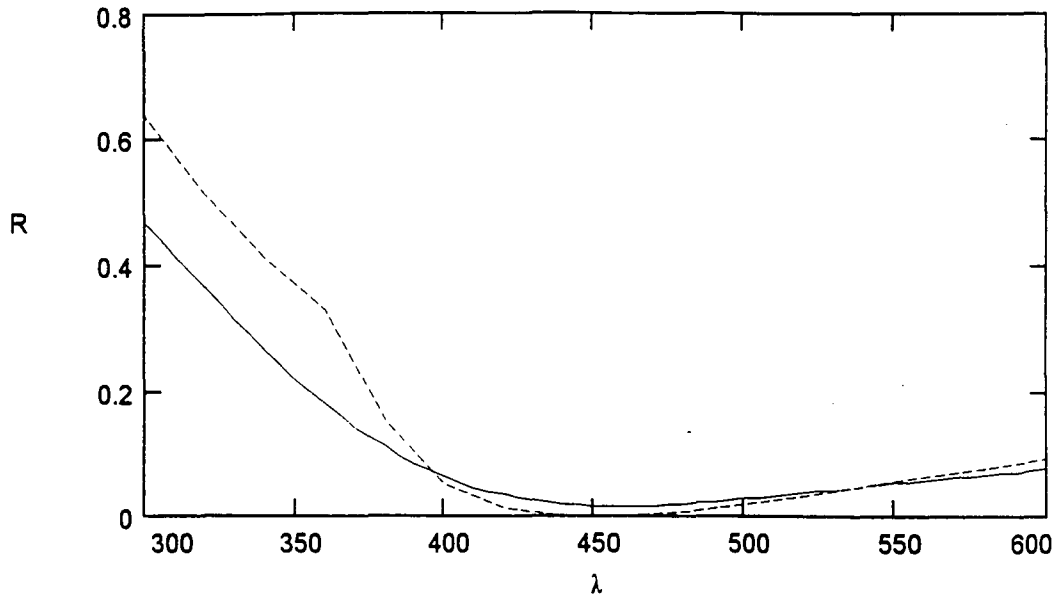

Figure 2 Reflectance (R) as a function of wavelength for Silicon Nitride on Silicon Theoretical - solid line Experimental - dashed line

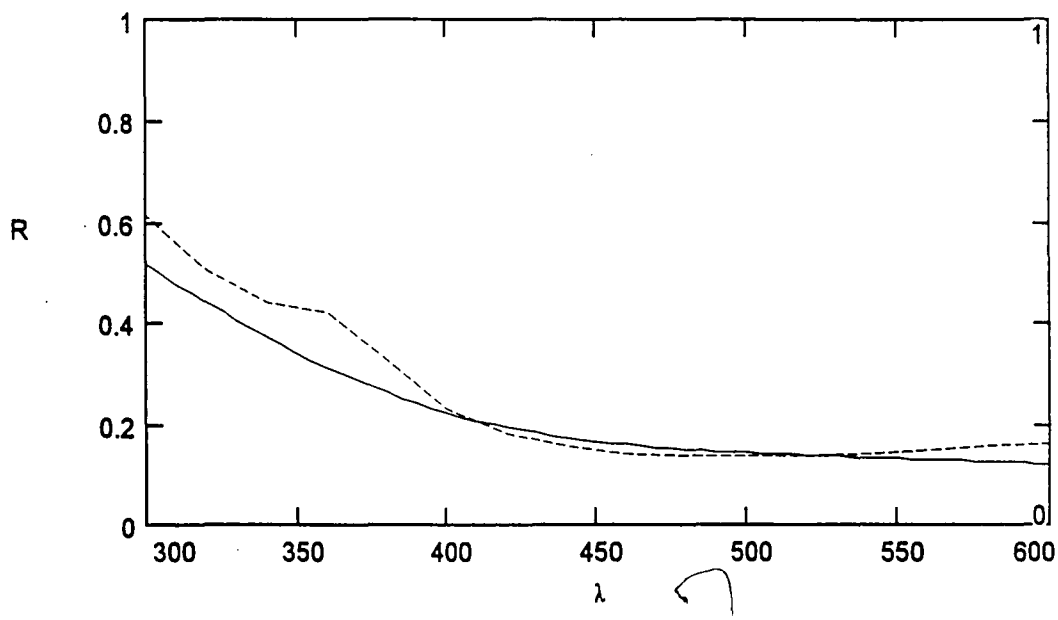

Figure 3 Reflectance (R) as a function of wavelength for Silicon Dioxide on Silicon. Theoretical - solid line Experimental - dashed line

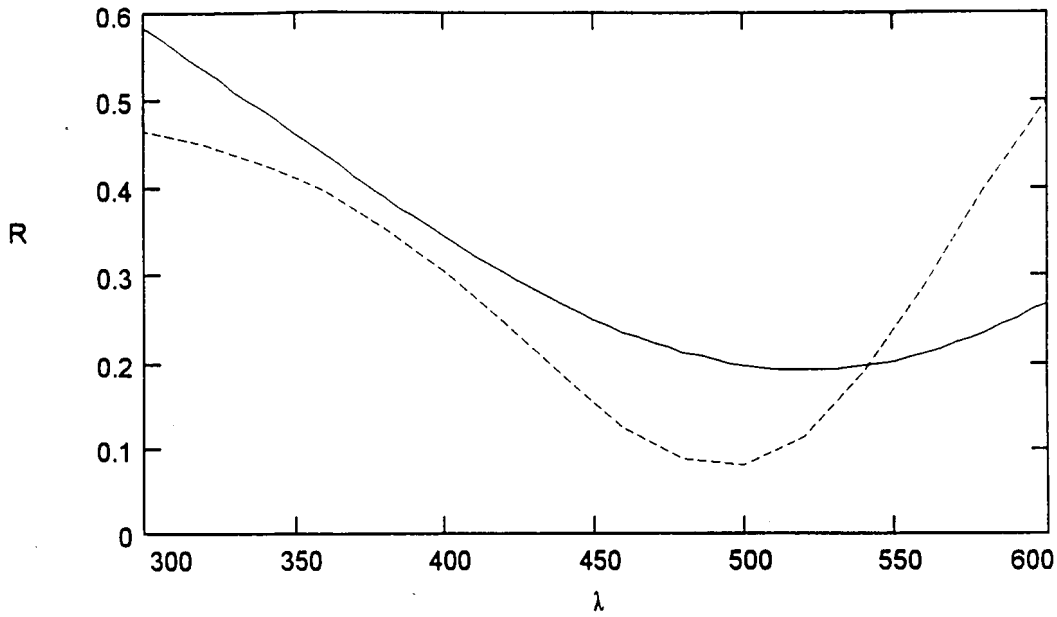

Figure 4 Reflectance (R) as a function of wavelength for amorphous silicon on Aluminum. Theoretical - solid line Experimental - dashed line

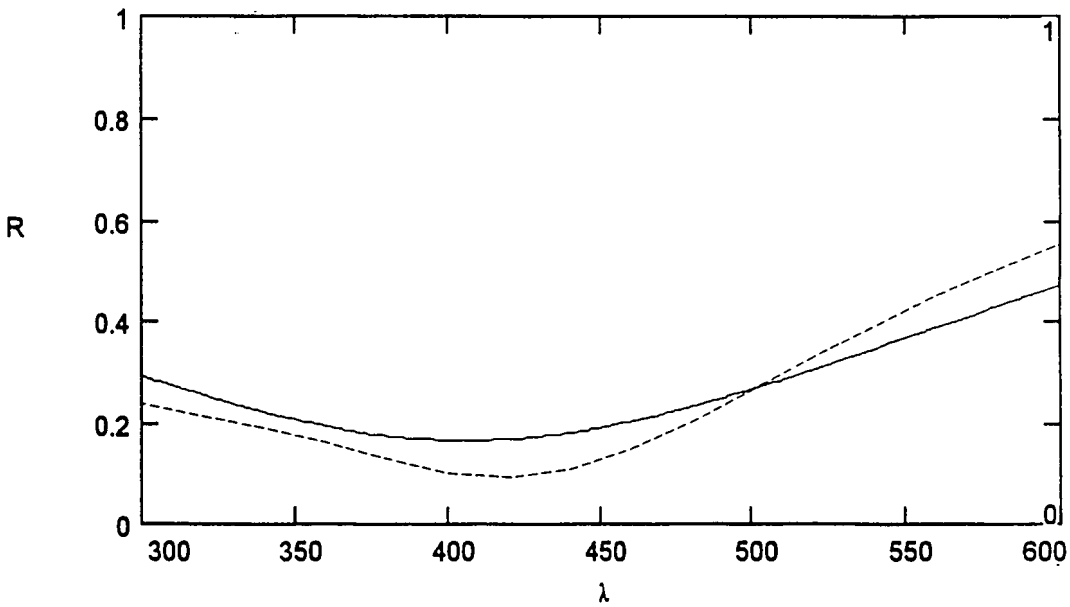

Figure 5 Reflectance (R) as a function of wavelength for titanium nitride on Aluminum. Theoretical - solid line Experimental - dashed line

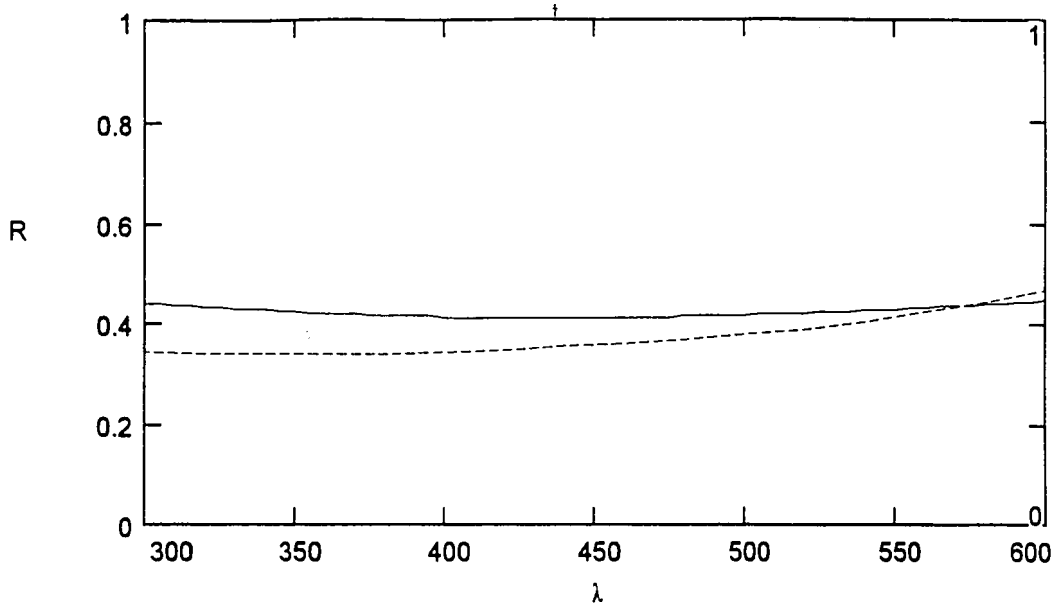

Figure 6 Reflectance (R) as a function of wavelength for tantalum silicide on aluminum. Theoretical - solid line Experimental - dashed line

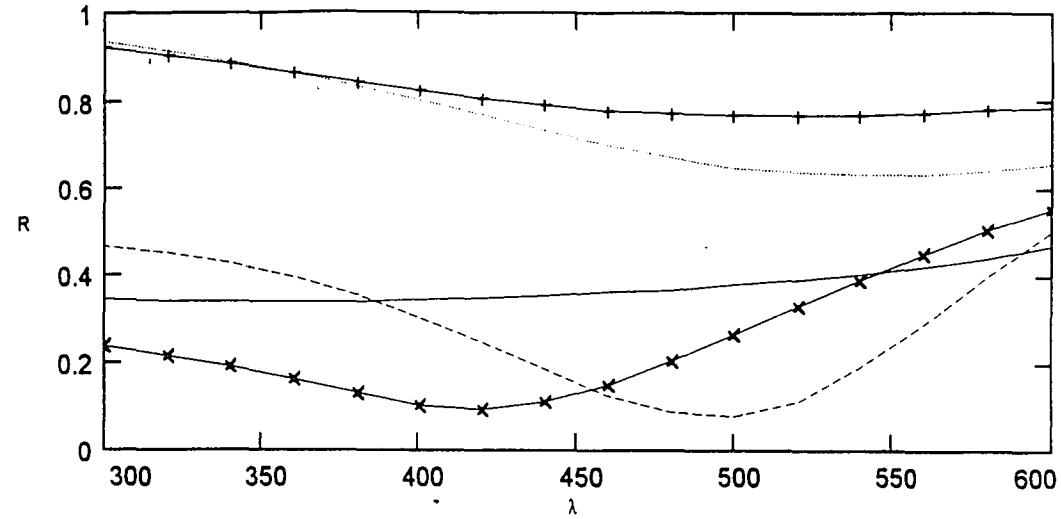

Figure 7 Comparison of Reflectance (R) for an aluminum substrate as a function of wavelength. Amorphous Silicon - dashed line; Tantalum Silicide - solid line; Titanium Nitride - --x-- line; Silicon Dioxide - --+-- line; Silicon Nitride - dotted line. With the exception of the silicon dioxide and silicon nitride curves, all data is from experimental measurement

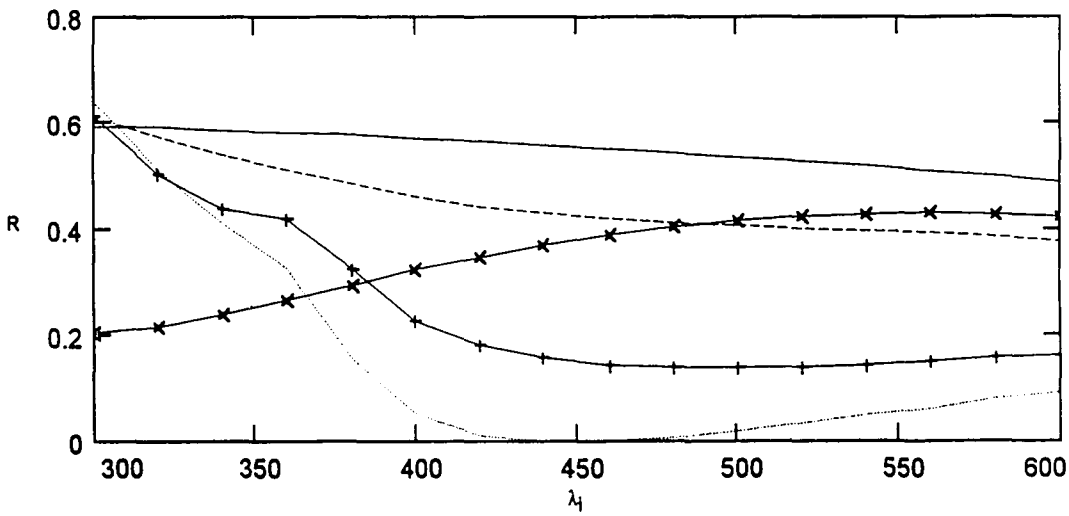

Figure 8 Reflectance comparison for a Silicon substrate as a function of wavelength. Amorphous silicon - dashed line; tantalum silicide - solid line; titanium nitride - --x-- line; silicon dioxide - --+-- line; silicon nitride - dotted line. With the exception of the silicon dioxide and silicon nitride curves all data is theoretical determination.

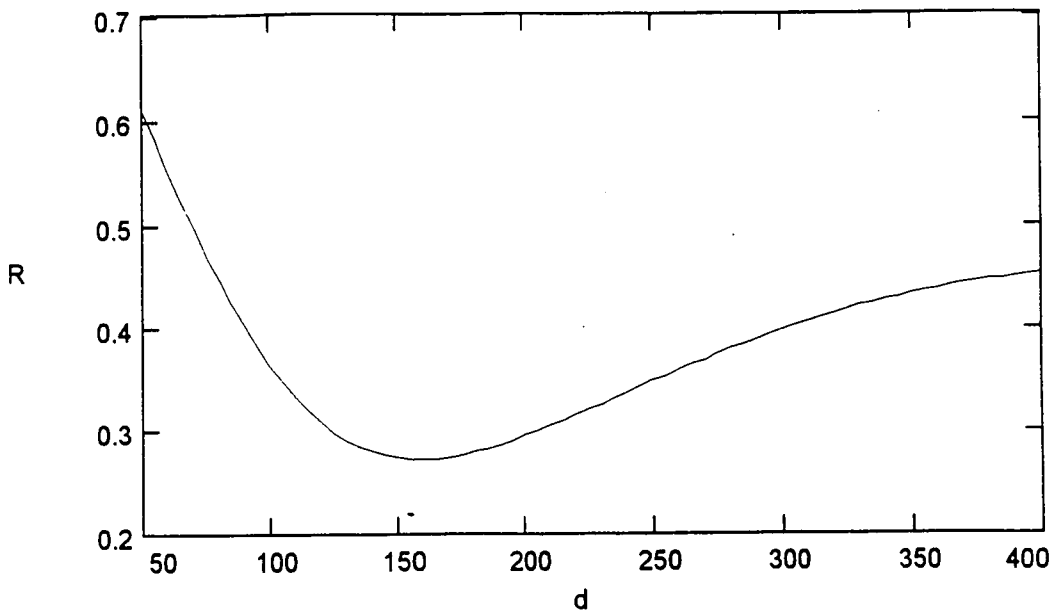

Figure 9 Reflectance (R) as a function of thickness (d) for amorphous silicon on Aluminum at 436nm.

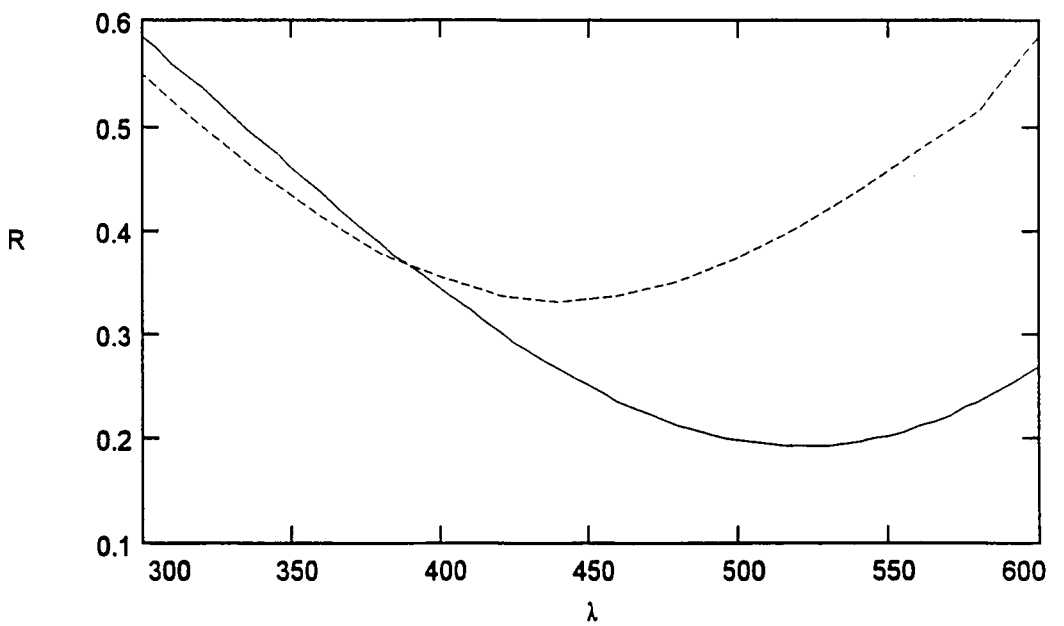

Figure10 Reflectance (R) as a function of wavelength for amorphous silicon on Aluminum. Thickness 160A - solid line
Thickness 110A - dashed line

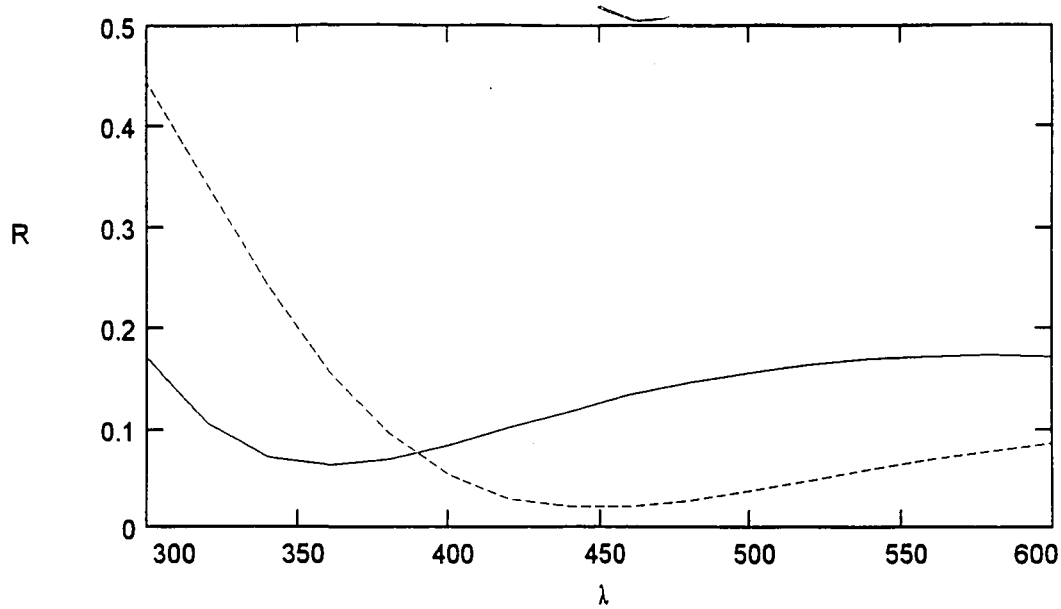

Figure 11 Reflectance (R) as a function of wavelength for silicon nitride on silicon Thickness 400A - solid line
Thickness 542A - dashed line

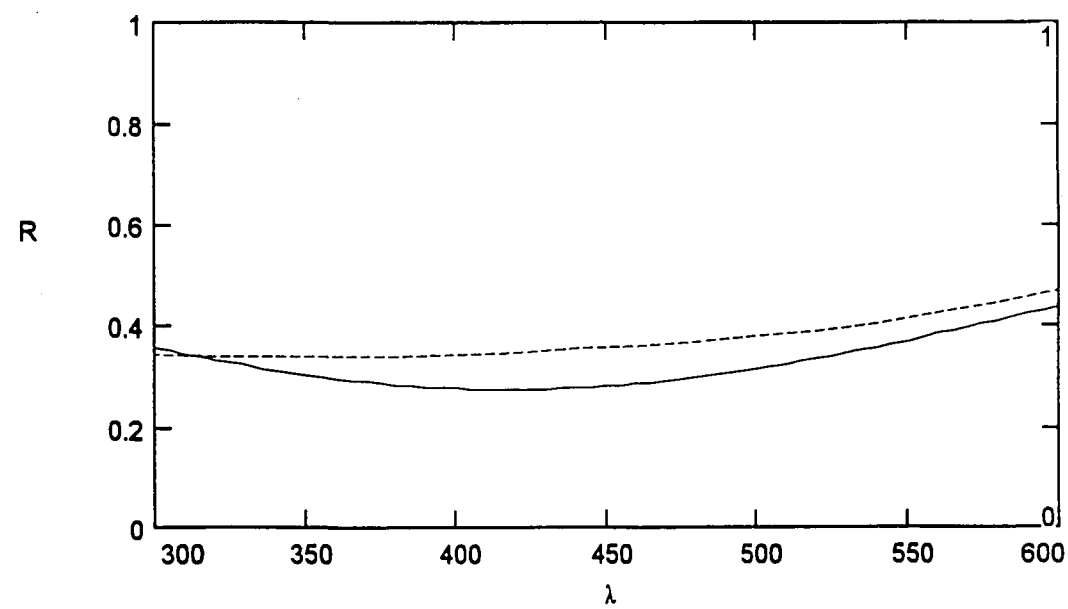

Figure12 Reflectance (R) as a function of wavelength for tantalum silicide on aluminum. Value obtained by Schneegans - solid line
Experimental - dashed line

Appendix A

For the case of a single absorbing layer on an absorbing substrate the following Fresnel equations are developed for reflectance. The following definitions apply to figure 9

n_0 = index of refraction for air
n_1 = index of refraction for the deposited layer
k_1 = the absorption coefficient for the deposited layer
n_2 = index of refraction for the substrate
k_2 = the absorption coefficient for the substrate
d_1 = thickness of deposited layer

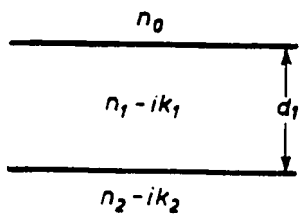

Figure 13 Single absorbing layer system

For the case of a non absorbing medium, such as Silicon Nitride, the value of k is null and can utilize the same series of equations.

Using these definitions allows for the following equation which determines reflectance as a function of wavelength. We shall denote the coefficients at the m^{th} interface as $r_m = g_m + ih_m$ and $t_m = 1 + g_m + ih_m$. From equation 14 and 15 the reflection and transmission at the two boundaries are described by

$$g_1 = \frac{n_0^2 - n_1^2 - k_1^2}{(n_0 + n_1)^2 + k_1^2} \qquad h_1 = \frac{2n_0k_1}{(n_0 + n_1)^2 + k_1^2}$$

$$g_2 = \frac{n_1^2 - n_2^2 + k_1^2 - k_2^2}{(n_1 + n_2)^2 + (k_1 + k_2)^2} \qquad h_2 = \frac{2(n_1k_2 - n_2k_1)}{(n_1 + n_2)^2 + (k_1 + k_2)^2}$$

As the radiation traverses the medium it undergoes a phase change of both its real and imaginary parts and is determined by the following.

$$p_2 = e^{\alpha_1} \cos\gamma_1 \qquad q_2 = e^{\alpha_1} \sin\gamma_1$$

where

$$\alpha_1 = \frac{2\Pi}{\lambda} k_1 d \qquad \gamma_1 = \frac{2\Pi}{\lambda} n_1 d_1$$

At the interface between the ARL and substrate an additional phase change is undergone by the incident wavefront. This is represented by

$$t_2 = e^{-\alpha_1} (g_2 \cos\gamma_1 + h_2 \sin\gamma_1)$$

$$u_2 = e^{-\alpha_1} (h_2 \cos\gamma_1 - g_2 \sin\gamma_1)$$

where

t_2 = the phase change at the substrate interface wrt n

u_2 = the phase change at the substrate interface wrt k

Using the previously defined equations depicting the incident and reflected waves the following equations are generated to represent the changes across the sample.

$$q_{12} = q_2 + h_1 t_2 + g_1 u_2$$

$$q_{12} = q_2 + h_1 t_2 + g_1 u_2$$

$$t_{12} = t_2 + g_1 p_2 - h_1 q_2$$

$$u_{12} = u_2 + h_1 p_2 + g_1 q_2$$

These equations when combined result in the effective reflectance produced by the system.

$$R_1 = \frac{t_{12}^2 + u_{12}^2}{p_{12}^2 + q_{12}^2}$$

Appendix B

Sample calculation of optical indices using Delta-Psi measurements for aluminum at 632nm

$$\Psi = 41.43 * (\frac{\Pi}{180})$$

$$\Delta = 135.31 * (\frac{\Pi}{180})$$

$$\Phi = 70 * (\frac{\Pi}{180})$$

$$n = \frac{-(\sin(\Phi) * \tan(\Phi) * \cos(2\Psi))}{(1 + \sin(2\Psi) * \cos(\Delta))}$$

$$k = \frac{(\sin(\Phi) * \tan(\Phi) * \sin(2\Psi) * \sin(\Delta))}{(1 + \sin(2\Psi) * \cos(\Delta))}$$

The complex index of refraction is then equal to

$$n = \sqrt{(n^2 - k^2) - i * (2nk)}$$

Which yields

$$n = 1.089 + 6.116i$$

References

1. Heavens O.S. "Optical Properties of Thin Solid Films" Dover publications, Inc. 1965.

2. B.L.Draper, A.R.Mahoney, G.A.Bailey, "Wavelength and Thickness-Independent Optical Coatings for Integrated Circuit Metallization Layers",J.Appl. Phys.62pp.4450-4452(1987).

3. M.Rocke, M.Schneegans, "Titanium Nitride for Antireflection Control and Hillock suppression on Al-Si Metallization",J.Vac.Sci.Techn.B6,pp.1113-1115(1988)

4. Rudloph Research AutoEL MŜ Manual, April 1989.

5. Perkin-Elmer UV/VIS/NIR Spectrophotometer Manual, May 1988.

6. C. Nolscher, L. Mader, M. Schneegans "High contrast single layer resists and antireflection layers - an alternative to multilayer resist techniques", SPIE Vol.1086, 1989, pp.242-250.

7. Garbuny M. "Optical Physics" Academic Press Inc. 1965.

Biography

Glenn A. Marshall was born in New Brunswick, New Jersey on December 15, 1962. He is the son of Helen and Ernest Marshall. He graduated from Middlesex County College in May 1984 with an Associates degree in Engineering Science. He then continued his education at Rochester Institute of Technology in Rochester, New York where he received a B.S. in Microelectronic Engineering. While at RIT he had Co-op assignments at RCA where he was involved with Radiation hardened device characterization and Computer assisted layout. He has been working with AT&T Microelectronics-Allentown since May 1988. He currently is a process engineer involved with the photolithography of sub-micron MOS devices.

END

OF

TITLE